Capturing the temperature gradients of GMAW hardfacing processes by employing CFD and FEM simulation procedures

Bogdan Marian Verdete[1], *Corneliu* Rontescu[2] , and *Tudor George* Alexandru[1*]

[1]University Politehnica of Bucharest, Department of Robots and Manufacturing Systems, 313 Splaiul Independenţei, Bucharest, Romania
[2]University Politehnica of Bucharest, Department of Quality Engineering and Industrial Technologies, 313 Splaiul Independenţei, Bucharest, Romania

Abstract. Hardfacing is carried out whenever a local improvement of the mechanical properties of metallic parts is demanded. In this regard, gas metal arc welding technology is one of the most popular choices. One decisive factor of the welded joint quality is governed by the heat affected zone. The present paper proposes a simulation methodology that can be employed for capturing the temperature gradients in any location of the base metal, when such information is required. The model was developed by using ANSYS Workbench simulation software and is based on coupled CFD and Transient Thermal analysis. In the first stage, a welded sample is subjected to 3D scanning for recreating its constitutive surfaces in a CAD environment. In the next stage, the convective heat transfer occurring due to the velocity of the shielding gas is captured by means of CFD analysis. Experimentally derived temperatures are employed for developing a transient thermal analysis, having defined the exterior heat transfer coefficient. In the last stage, the simulation results are verified in an arbitrary location of the base metal that is located outside the heat affected zone.

1 Introduction

According to ISO/TR 13393, hardfacing represents the deposition of a metallic alloy onto a substrate, in view of achieving enhanced mechanical properties at the level of the base metal [1]. This process can be carried out by means of gas, arc, powder spraying, or laser welding processes [2]. The resulting product is characterized by superior wear resistance. Examples of applications are depicted throughout the literature in all major industrial fields, such as aerospace and automotive [3]. Gas metal arc welding (GMAW) is one of the most common hardfacing technologies, given its high productivity and low costs [4]. A limiting aspect of this process is emphasized by the existence of a heat affected zone in the proximity of the build-up layers [5]. In this regard, the study of the heat transfer occurring at the welded joint levels is required to ensure the quality of the end product. Only a limited

* Corresponding author: alexandru_tudor_imst@yahoo.com

range of papers are published related to the subject. In [6], the authors describe an approach for capturing the temperature distribution in GMAW hardfacing by employing Computational Fluid Dynamics (CFD) on a simplified model. The mesh was generated by using polyhedral elements. Multiphase flows have been substituted by thermal effects of liquid metal transport, melting, solidifying and allotropic changes. Another approach that is applicable to the thermal analysis of GMAW hardfacing is depicted in [7]. The paper describes a simulation approach that is based on SysWeld Finite Element Method (FEM) simulation software. In the first stage, a reduced order model is developed by employing a 2D simulation procedure. Modeling of the heat sources is completed by employing the Goldak temperature model. The results achieved capture the dynamics of the process in the vicinity of the heat affected and molten zones. Other paper that relates to the subject is described in [8]. The approach is based on the 3D CFD analysis package ArcWeld. In the present research, the authors propose a new simulation procedure that combines CFD analysis for capturing the forced convection heat transfer and FEM transient thermal simulations for processing the time vs. temperature graphs. The geometry of the base metal and welded joint is derived from 3D scanning of real-world samples. Infrared thermography is carried out a priori for evaluating the temperatures of the welded joint. A good match was noticed between the experimental vs. simulation temperature curves. Opposed to the existing approaches, the present work can recreate the full dynamics of GMAW hardfacing heat transfer, including phenomenon such as arc instability. This is achieved due to the direct use of experimental data for developing the simulation model. On the other hand, the coupling of CFD and FEM thermal analysis combined with the effective use of the element birth and death technique lowers the computational demands of the problem. Thus, the influence of any welding parameters or environmental conditions on the thermal behavior of the GMAW hadfacing process can be studied through the further use of the methodology.

2 The proposed approach

The proposed approach consists of 4 layer of abstraction. The interaction between them is depicted in figure 1.

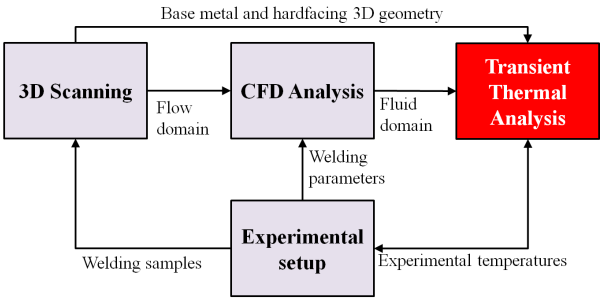

Fig. 1. Schematic representation of the proposed approach.

The experimental setup supports the simulation model development and verification stages. Welding samples are provided for both virtual prototyping and temperature acquisition purposes. The conversion of the physical base metal and welded joint geometry into a three-dimensional model is carried out by employing 3D scanning techniques. CFD analysis is employed for capturing the fluid domain of the GMAW hardfacing process. The resulting geometry, the description of the fluid domain and the experimentally derived

temperatures are used as input data for developing the transient thermal analysis. All of these aspects are discussed in-depth in the sub-sections below.

2.1 The experimental setup

In the first stage, an experimental setup is developed to analyze the temperature distributions occurring at the level of a sheet metal that is subjected to GMAW hardfacing. The material employed is S235JR steel (according to EN ISO 10025-1:2005), the dimensions of the work piece being 200x100x10 mm.

A robotic cell is employed for completing the welding process. In this regard, a Fanuc ARC Mate 100iB industrial robot that is equipped with a Fronius RA5000 torch is used. According to EN ISO 14341:2010, the electrode wire has a chemical composition (C=0.078%, Si = 0.85, Mn = 1.5%), that is like the base metal. Its diameter is 1.2 mm of SG2 type. The shielding gas used is a mixture of Ar (82%) and CO_2 (18%).

Table 1 depicts the most relevant welding parameters.

Table 1. The choice of welding parameters.

Parameter	Symbol	Value	Unit of measurement
Shielding gas flow rate	v_g	10	l/min
Welding current	I	320	A
Voltage	U	31.7	V
Wire feed speed	V_{fs}	11	m/min
Welding speed	V_s	55	cm/min
Nozzle to work distance	l	20	mm

An in depth overview of the welding cell and the experimental setup employed for capturing the temperatures of the GMAW hardfacing process is presented in figure 2.

Fig. 2. Details regarding the robotic welding cell and the experimental setup.

In figure 2, the industrial robot and its dressing equipment (1) carry out the GMAW process at the level of the work piece (5) that is secured in place by a welding fixture (6). Two non-contact temperature acquisition systems are included: A FLIR Thermacam SC640

infrared thermography camera (4) and a Raytek Raynger MX4 Infrared Thermometer (2). An acquisition PC (3) is used for recording the values. This experimental approach was adopted to cover two temperature ranges that occur during the process:

- **Acquisition interval between 400 and +2000°C:** are captured by employing the thermography camera. These temperatures occur on the exterior surfaces of the welded joint during the melting and solidification stages. The measured values are processed in individual sections of the welded joint (by considering a 5 mm pitch).
- **Acquisition interval between -50 and +800°C:** are captured by employing the infrared thermometer. These temperatures are measured outside the working area (presented in figure 3, in the upper left corner of the base metal).

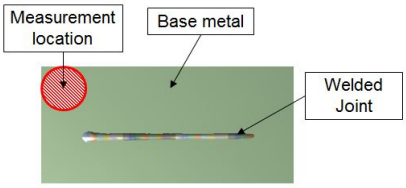

Fig. 3. Infrared thermometer temperature acquisition location.

While the resulting values have no direct contribution to the development of the simulation model, they can prove useful for verifying the accuracy of the transient thermal analysis (given the fact that both conductive and convective heat transfer mechanisms occur in that location).

2.2 The 3D scanning procedure

3D scanning involves reconstructing the exterior surfaces of a physical body by mapping the location of characteristic points with the support of image processing techniques. For the present study, the physical welded sample was subjected to the 3D scanning process (Fig.4–a) by employing a 7-axis Absolute Arm (1).

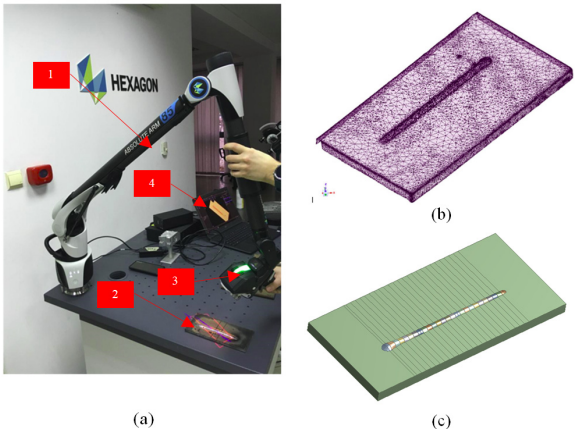

Fig. 4. The 3D scanning process and the resulting three-dimensional model.

The procedure involves positioning the work piece (2) on a rigid table. A laser scanner (3) is attached to the arm to ensure its optimal stiffness during the manual acquisition procedure. A PC (4) is used to process the output coordinates of characteristic points. The

stereolitographic shape of the 3D body (Fig.2-b) is generated with the support of Inspire metrology software.

In the next stage, the scanned cloud data is imported into ANSYS Workbench for geometry clean up. The SpaceClaim interface is employed for this purpose. In this regard, the exterior surfaces of the welded joint are delimited from the base metal. Topological operations are carried out to materialize the individual volumes (Fig.2-c). Thus, the processed model can be further use for developing both CFD and FEM simulations. The welded joint is sliced in 27 sections, each one having a spacing of 5 mm. In this way, a better control of the mesh strategy can be achieved.

2.3 The CFD analysis

CFD analysis represents a branch of fluid mechanics that makes use of mathematical models and algorithms for solving fluid flow problems. The Navier-Stokes equations are employed, equations which describe the relationship between density, temperature, velocity and pressure of a moving fluid. The equations that are used to model the flow of fluids are based on the laws of mass, impulse and energy conservation. The relationships 1-3 are derived from [9].

Equation 1 represents the general form of mass conservation or continuity:

$$\frac{\partial p}{\partial t} + \nabla \cdot \left(\rho \cdot \vec{v} \right) = S_m \tag{1}$$

Where: ρ represents the density of the fluid, $\vec{v}$ the velocity vector and S_m the source mass.

The conservation of momentum in an inertial reference frame is described in equation 2:

$$\frac{\partial}{\partial t}\left(\rho \cdot \vec{v} \right) + \nabla \cdot \left(\rho \cdot \vec{v} \cdot \vec{v} \right) = -\nabla_p + \nabla \cdot \left(\bar{\bar{\tau}} \right) + \rho \cdot \vec{g} + \vec{F} \tag{2}$$

Where: p represents the static pressure, $\bar{\bar{\tau}}$ the stress tensor, $\rho \cdot \vec{g}$ the gravitational body force and $\vec{F}$ the external body forces.

$$\frac{\partial}{\partial t}\left(\rho E \right) + \nabla \cdot \left(\vec{v} \cdot \left(\rho E + \rho \right) \right) = \nabla \cdot \left[\left(k_{eff} \nabla T \right) - \sum_j h_j \vec{J}_j + \left(\bar{\bar{\tau}}_{eff} \cdot \vec{v} \right) \right] + S_h \tag{3}$$

Where: $k_{eff}=k_k + k_c$ is the effective conductivity, k_t is the turbulent thermal conductivity, defined in accordance with the turbulence model employed, and $\vec{J}_j$ the diffusion flux of species. In equation 3, the first three terms represent the energy transfer due to conduction, species diffusion and viscous dissipation. S_h takes into account any other volumetric heat sources. Additional transport equations are employed in case of turbulent flow.

The objective of the CFD analysis is to capture the velocity and pressure of the shielding gas and its interaction with the welded joint. The aim of the simulation is to evaluate the forced convection heat transfer coefficients that occur on the exterior surfaces of the model. ANSYS Fluent is employed for this purpose. The resulting values are exported in CSV files, being further use for developing the transient thermal analysis.

The simulation model takes into account a flow domain that is delimited by walls. The nozzles of the welding torch are explicitly modeled for taking into account the flow of the shielding gas. Analytical calculations are carried out for identifying its velocity:

$$v_g = \frac{Q}{A} \tag{4}$$

Where: v_g represents the velocity of the gas [m/s]; Q represents the gas flow [m^3/s] and A the average circumference of the nozzle [m^2].

For the given problem, v_g = 1.08 m/s.

Figure 5 depicts the definition of the simulation domain.

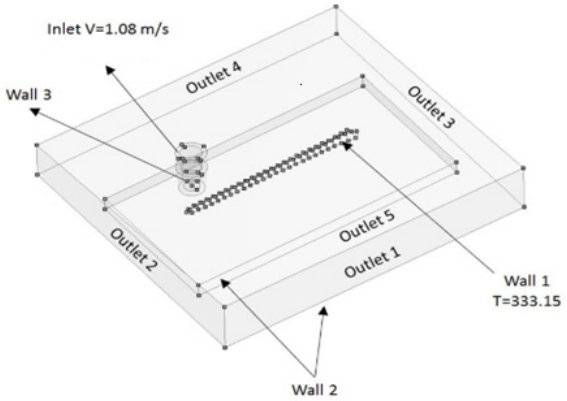

Fig. 5. The inlet, outlet and wall locations of the fluid domain.

The shielding gas flows at a temperature of 18°C (the ambient temperature measured during the experimental procedure). Walls are positioned in the proximity of the welded joint and at the tip of the torch. All other areas are considered outlets.

The k-ε turbulence model is employed, given the Reynolds number that is about $1.00 \cdot 10^5$ for this problem. Energy equations are activated and the near-wall temperature result option is employed for exporting the forced convection film coefficient.

Figure 6 depicts the velocity of the shielding gas when the torch is positioned in the center of the welded joint.

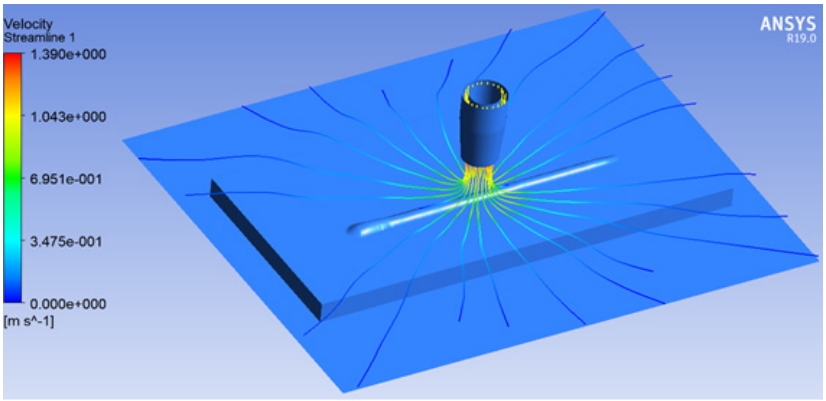

Fig. 6. The velocity streamline captured in the middle position of the torch.

The maximum value of 1.39 m/s occurs in the interior of the nozzle. On the other hand, a fluid velocity of about 0.7 m/s can be noticed at the gas-welded joint interaction area.

Figure 7 depicts the change of the forced convection film coefficient in relation to the position of the welding torch.

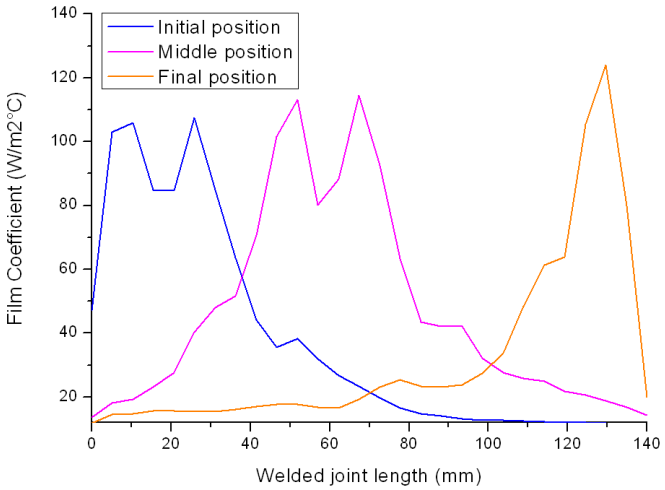

Fig. 7. The forced convection film coefficient vs. the welded joint length.

The graph from figure 7 emphasizes the influence of the welded joint on the value of the convection film coefficient. This is due to the turbulent regime that occurs in that area. In this regard, the maximum values occur in the final stage of the welding cycle (~120 W/m^2°C).

2.4 The transient thermal analysis

The transient thermal analysis is carried out to evaluate the temperature distribution and total heat fluxes that occur in a structure by considering time varying loads. In FEM software, the heat transfer by conduction, convection and radiation can be simulated for beams, shells and solids that are in contact with a layer of fluid. These elements are characterized by a single degree of freedom, the nodal temperatures.

The specific heat is required to evaluate the heat that is stored in the base metal and welded joint [10]:

$$[C]_i \cdot \{\dot{T}\}_{i+1} + [K]_i \cdot \{T\}_{i+1} = \{Q\}_i \tag{5}$$

Where: [C] represents the specific heat matrix, [K] represents the thermal conductivity matrix, {T} the nodal temperature vector and Q the vector of the effective nodal heat flux.

The analysis is completed by defining the fluid and solid domain of the problem:

- **Solid domain:** materializes the heat transfer that occurs due to conduction. In this case, thermal energy is dissipated from the weld pool to the adjacent cold plate. Due to the dynamics of the process, only a fraction of the total energy is stored in the base metal, resulting an internal temperature gradient. The ability of the work piece to store heat is influenced by the specific heat and density of the material. The initial temperatures are defined as prescribed ones for each section of the welded joint. These values are derived from the data acquired from the infrared thermography camera.

- **Fluid domain:** materializes the interaction between the base metal, welded joint and the surrounding environment. Two heat transfer mechanisms can be distinguished: forced convection (occurring due to the velocity and displacement of the shielding gas – derived from the CFD analysis) and natural convection (occurring due to the stagnant air of the industrial environment).

The temperatures of the welded joint are defined for each of its individual sections based on the experimental data derived in the previous stage. Figure 8 emphasizes the resulting values for the initial, middle and final position of the welding torch.

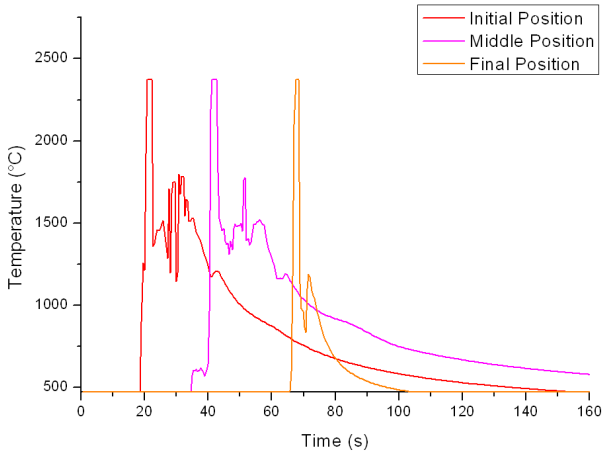

Fig. 8. Experimental temperatures derived for the initial, middle and final position of the torch.

Due to the fact that the acquisition procedure also captures the temperatures of the arc, a filtering technique is required to remove the parasitic values. An approach based on histograms is proposed in figure 9.

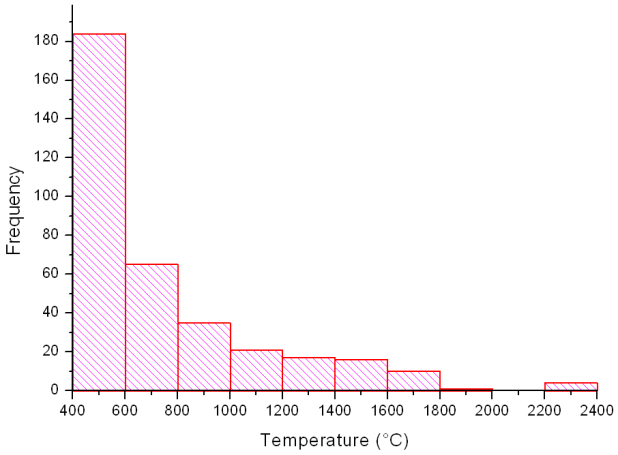

Fig. 9. Skew right type histogram of the experimental temperatures for the middle position of the torch.

The example is provided for the middle position of the welding torch. In this case, the distribution type matches the skew right type. A discontinuity of the experimental values can be noticed between 1800 and 2200°C. These data points have a low number of specimens and occur only due to the welding arc and its instability. To filter these sources of noise, an average of the last bin with continuous values is carried out (1600 and 1800 in

the example provided). In this regard, table 2 represents the maximum temperatures of the welded joint for the initial, middle and final position of the torch.

Table 2. The resulting temperatures after processing the histogram

Position of the welding torch	Initial	Middle	Final
Temperature (°C)	1708^0C	1463^0C	1188^0C

Based on the welding speed of 55 cm/min, the total welding time is 14.8 seconds. A cool down cycle of 145.2 seconds is considered to capture the full dynamics of the process.

Due to the fact that material is added to the system during the hardfacing process, the element birth and death option is employed to activate groups of elements in accordance with the welding parameters. In this regard, the progressive generation of the welded joint is achieved by multiplying the conductivity of different welded joint sections with a severe reduction factor of $1 \cdot 10^{-6}$. For this purpose, the total simulation time was divided in equal substeps of 0.55s. This value was derived from the welding speed and length of the welded joint. All sections are considered initially "dead" and are turned on in accordance with the trajectory of the torch. This approach can be materialized by a 27x27 matrix A:

$$A = \begin{Bmatrix} 0 & 1 & 1 & 1 & \dots & 1 \\ 0 & 0 & 1 & 1 & \dots & 1 \\ 0 & 0 & 0 & 1 & \dots & 1 \\ 0 & 0 & 0 & 0 & \dots & 1 \\ \vdots & \vdots & \vdots & \vdots & \dots & \vdots \\ 0 & 0 & .. & .. & .. & 1 \end{Bmatrix} \tag{6}$$

Where: each row represents a time step while each column represents an individual welded joint section. For example, for a_{11}, the section number is 1 and the simulation time is 0.55 seconds. When the value of a_{11} is 0, the corresponding section is "dead", and "alive when a_{11} is 1.

The results of the simulation model are presented in figure 10 for the temperature distribution occurring in the initial position of the torch.

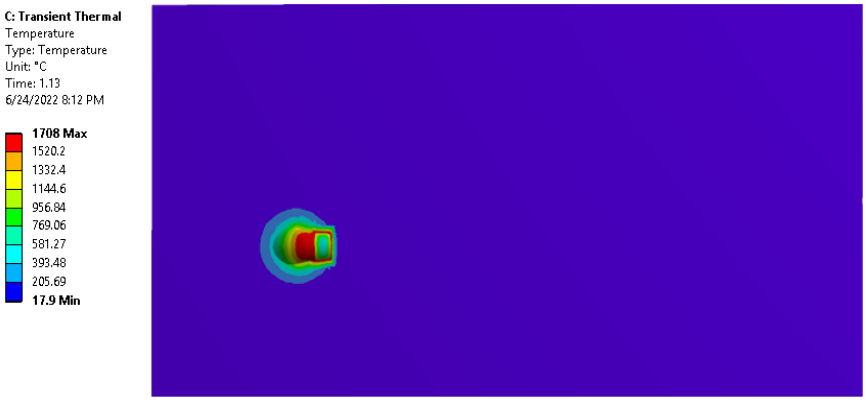

Fig. 10. The temperature distribution in the base metal at the begging of the welding cycle.

In this case, the maximum temperature of 1708°C is localized in the proximity of the weld pool. A thermal gradient can be noticed due to the conduction of the base metal.

Initially, only a small fraction of the generated heat is stored in the work piece. A more significant gradient is emphasized by the end of the welding cycle (Fig.11).

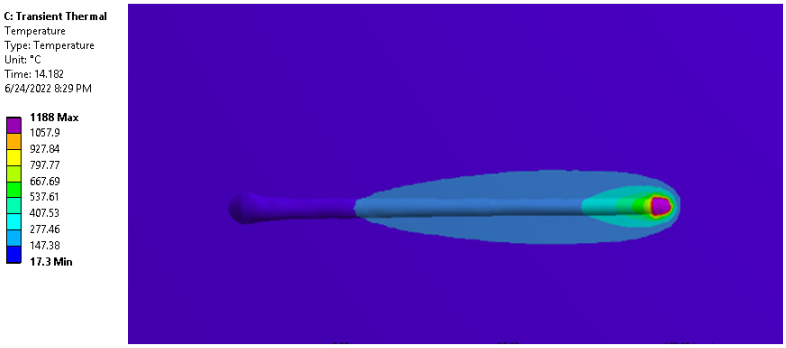

Fig. 11. The temperature distribution in the base metal at the end of the welding cycle.

The welded joint cools down due to the forced convection that is caused by the shielding gas (until 14.8 seconds). Afterwards, natural convection becomes the dominant heat transfer mechanism. (Fig. 12)

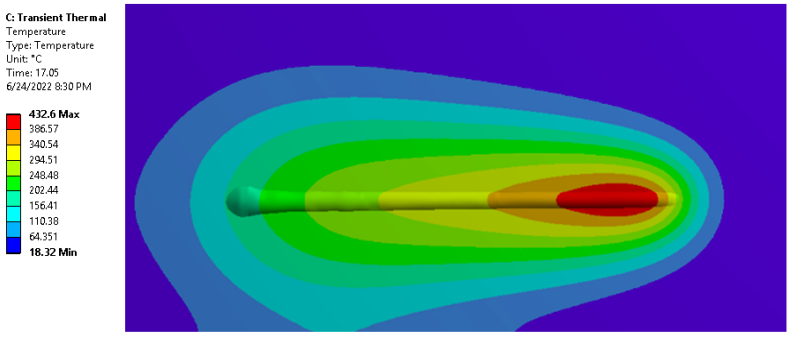

Fig. 12. The temperature distribution in the base metal under natural convection.

For information, figure 13 illustrates the temperature distribution of the work piece after 157.4 seconds.

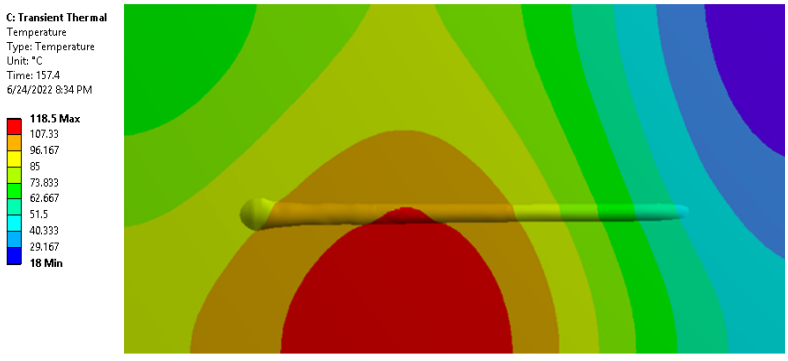

Fig. 13. The temperature distribution after 142.6 seconds of cool down.

In this case, the maximum value is 118.5°C.

Results from the upper-left corner (see Fig. 3 for information) are processed as a time vs. temperature graph (Fig.14).

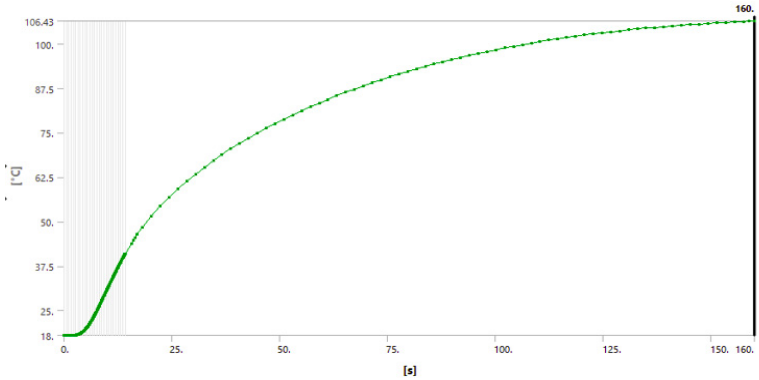

Fig. 14. Results in the upper-left corner of the base metal derived from the Transient Thermal analysis.

The experimentally derived values achieved by means of the infrared thermometer are further used to verify the accuracy of the simulation model. In this regard, the values that were measured in the upper right corner of the base metal are compared with the ones resulting from the transient thermal analysis (Fig 15).

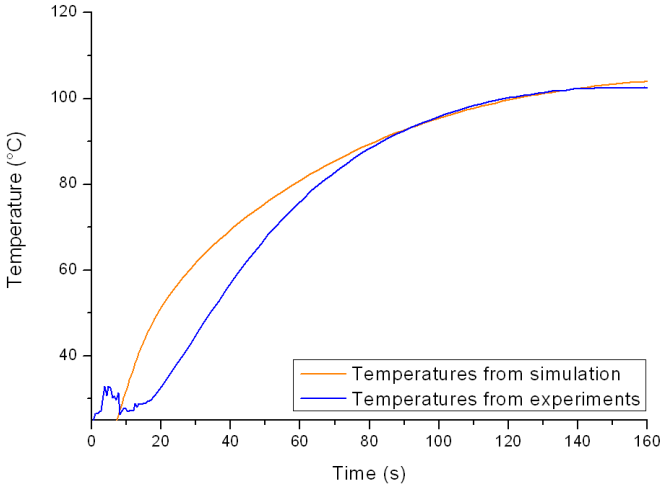

Fig. 15. Comparison between experiments and simulations in the upper-right corner of the base metal.

A good match can be noticed between the two curves, the steady-state error being estimated as 1.17%. On the other hand, the settling time error is about 5.18%.

3 Conclusion

The present paper presents an approach that is applicable to the thermal analysis of GMAW hardfacing, by employing CFD and FEM analysis procedures. For this purpose, an experimental setup comprising a robotic welding cell, an infrared thermography camera and an infrared pyrometer is employed. The simulation model is based on the coupling of two different physics: heat transfer and fluid flow. In this regard, CFD analysis captures the turbulent flow regime in the proximity of the welded joint. The forced convection film coefficient is calculated based on the average wall temperature. Furthermore, the transient thermal analysis evaluates the ability of the base metal to store heat due to the GMAW

hardfacing process, providing valuable information regarding the temperature profile in any location of the model. Therefore, the approach can successfully be employed for the study of the thermal influence of welding parameters or environmental conditions on the heat transfer dynamics of the GMAW hardfacing process. A discrepancy can be noticed when comparing the experimental vs. simulation curves. This is due to the fact that the experimental procedure was not perfectly synchronized with the time step settings employed in the transient thermal analysis. Even so, a good match was noticed between the slopes of the two curves.

The original contribution consists of:

1. Reverse engineering 3D scanned models
2. Coupling CFD and FEM analysis for capturing both thermal and fluid domains
3. Processing temperature acquisition noise by means of histograms
4. The use of the element birth and death technique for generating the welded joint
5. The use of experimental data for both model preparation and result verification.

Future work will focus on developing an automated procedure for synchronizing the temperature acquisition procedure with the working program of the robotic cell. Furthermore, improvements can be carried out regarding the filtering of noisy data for achieving a better comparison between the experiments and simulations.

References

1. F.C. Campbell, *Elements of metallurgy and engineering alloys*., 391-410 (2008)
2. G.R.C. Pradeep, A. Ramesh, B.D. Prasad, International Journal of Engineering Science and Technology, **2**(11), 6507-6510 (2010)
3. M.K. Saha, S. Das, Journal of the Association of Engineers, **86**(1-2), 51-63 (2010)
4. R.R. Garbade, N.B. Dhokey, Materials and Applications in IOP Conference Series: Materials Science and Engineering, **1**(1017), 1-10 (2020)
5. F. Schreiber, B. Allebrodt, T. Erpel, Zavarivanje i zavarene konstrukcije, **64**(1), 11-21 (2019)
6. A. Sachajdak, J. Sloma, I. Szczygiel, Applied Thermal Engineering, **141**, 378-385 (2018).
7. R. Konár, M. Mician, M. Málek, J. Šutka, M. Gucwa, J. Winczek, Journal of Applied Mathematics and Computational Mechanics, **20**(1), (2021)
8. D.W. Cho, J.H. Park, H.S. Moon, International Journal of Heat and Mass Transfer, **139**, 848-859 (2019)
9. ANSYS INC, ANSYS FLUENT Theory Guide 16.1 Documentation, April 2015
10. C. Pupăză, R.C. Parpală, *Modelare şi analiză structurală cu ANSYS Workbench*, 74-76 (2011)